OPEN ACCESS
ARTICLE
Journal homepage: www.the-innovation.org/energy-use
Energy Use
INNOVATION PRESS
Energy Use 2 (2026):100058
Contents lists available at INNOVATION PRESS

Effects of Street Orientation and Canyon Geometry on Thermal Improvement Efficiency of Retractable Sunshade Canopies at Pedestrian Level

Zongzhou Zhu,[1,*] Dan Wang,[1] Chaoyi Ma,[1] Chuan Ma,[2] Zeqin Wu,[3] and Xiaofei Han[4,*]
*Correspondence: zhu0527@nwpu.edu.cn (Z. Z.); s2118521@siswa.um.edu.my (X. H.)
Received: June 8, 2026; Accepted: June 22, 2026; Published Online: June 25, 2026; https://doi.org/10.59717/ipj.energy-use.2026.100058
© 2026 The Author(s). This is an open access article under the CC BY license (https://creativecommons.org/licenses/by/4.0/).

GRAPHICAL ABSTRACT

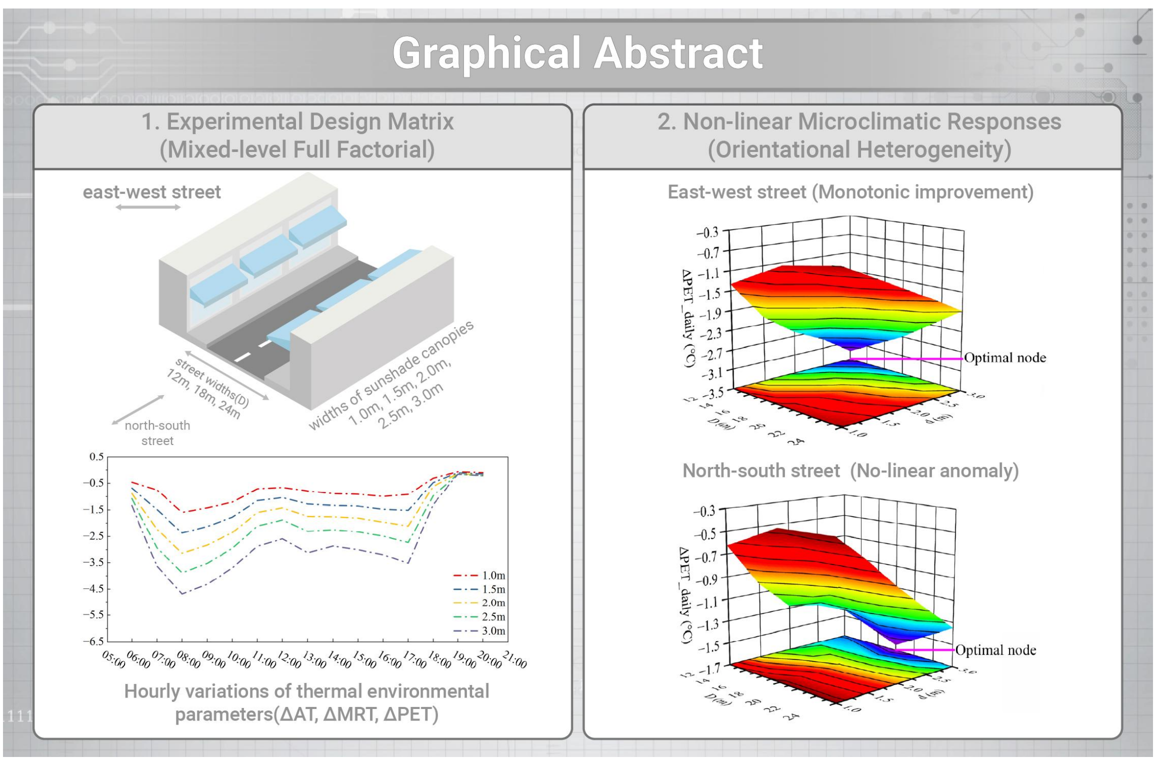

PUBLIC SUMMARY

- 36 ENVI-met summer solstice scenarios simulate hourly AT, MRT & PET (6:00–20:00) for retractable building sunshades with varied street orientations, widths and canopy lengths.
- Retractable canopies cut daily average PET by up to 4.67°C, mitigating extreme summer heat harm to residents and lowering buildings' cooling energy demand.
- E-W streets see linear thermal relief with longer canopies; 12m narrow streets with 3.0m canopies deliver the strongest cooling effect.
- 12m N-S streets with full-length canopies trap excess heat; the optimal N-S setup is 18m width + 3.0m canopies (max PET drop: -1.65°C).
- Dynamic adjustable shading systems are superior to static fixed layouts for balancing pedestrian thermal comfort and building cooling loads.

Journal homepage: www.the-innovation.org/energy-use
Energy Use
INNOVATION PRESS
Energy Use 2 (2026):100058
Contents lists available at INNOVATION PRESS

Effects of Street Orientation and Canyon Geometry on Thermal Improvement Efficiency of Retractable Sunshade Canopies at Pedestrian Level

Zongzhou Zhu,[1,*] Dan Wang,[1] Chaoyi Ma,[1] Chuan Ma,[2] Zeqin Wu,[3] and Xiaofei Han[4,*]
[1]School of Mechanics and Transportation Engineering, Northwestern Polytechnical University, Xi'an 710129, China
[2]Centre for Environment and Ageing Well, College of Design and Engineering, National University of Singapore, Singapore 119077, Singapore
[3]Advanced Home Futures, MIMA School of Art and Design, Teesside University, Middlesbrough TS1 3BX, UK
[4]Centre for Building, Construction & Tropical Architecture, Faculty of Built Environment, Universiti Malaya, Kuala Lumpur 50603, Malaysia
*Correspondence: zhu0527@nwpu.edu.cn (Z. Z.); s2118521@siswa.um.edu.my (X. H.)
Received: June 8, 2026; Accepted: June 22, 2026; Published Online: June 25, 2026; https://doi.org/10.59717/ipj.energy-use.2026.100058
© 2026 The Author(s). This is an open access article under the CC BY-NC-ND license (https://creativecommons.org/licenses/by/4.0/).
Citation: Zhu Z., Wang D., Ma C., et al. (2026). Effects of Street Orientation and Canyon Geometry on Thermal Improvement Efficiency of Retractable Sunshade Canopies at Pedestrian Level. *Energy Use* **2**:100058.

The extremely hot summer in China significantly exerts adverse impacts on residents' health and intensifies building cooling energy demands. This study quantifies the thermal effects of building-mounted, retractable sunshade canopies at the pedestrian level. Hourly values (6:00–20:00) of air temperature (AT), mean radiant temperature (MRT), and physiological equivalent temperature (PET) of 36 designed scenarios on the summer solstice were simulated via the ENVI-met software. The designed experimental scenarios integrated two street orientations (east-west and north-south), three street widths (D = 12, 18, 24 m), and five sunshade canopy lengths (d = 1.0, 1.5, 2.0, 2.5, 3.0 m). The results demonstrate that sunshade canopies can effectively improve the localized thermal environment, resulting in a maximum diurnal average PET reduction of 4.67°C. In the east-west street canyons, thermal mitigation effects exhibit a monotonic linear relationship with street canopy extension, with the peak efficiency occurred in the minimum D (12 m) coupled with the maximum d (3.0 m). A distinct adverse "heat retention" anomaly occurs in narrow north-south street (12 m wide) with maximal canopy length. Consequently, for north-south streets the optimal diurnal PET strategy shifts from the narrowest configuration to a medium D (18 m) combined with the maximum d (3.0 m), delivering a maximum local thermal comfort improvement corresponding to a PET reduction of -1.65°C. These empirical findings demonstrate the need to shift from rigid, static geometric layouts to dynamic and responsive shading regulation frameworks. This approach can synergistically optimize pedestrian-level outdoor thermal environment and cooling energy use of adjacent building.

INTRODUCTION

Global warming has become one of the most significant environmental challenges around the world. Since the mid-20th century, there has been an undisputed warming trend in the global climate system, accompanied by a significant increase in the frequency, duration, and severity of extreme heat anomaly events.[1] The predictions outlined in the Sixth Assessment Report of the Intergovernmental Panel on Climate Change indicate that continued greenhouse gas emissions will inevitably exacerbate these extreme temperature events throughout the 21st century. As the country with the fastest urbanization process in the world in recent decades, China has experienced a continuous increase in the risk of compound heatwaves and droughts in most areas from 1961 to 2020, exacerbating the environmental disaster threat faced by urban residents.[2] The 2025 China Climate Bulletin pointed out that the annual average temperature in the country is still continuing to rise steadily, and the frequency and intensity of extreme heat events are also increasing, further confirming corroborating this long-term warming trend.[3]

Extreme thermal exposure has evolved into a critical public health crisis, particularly in high-density metropolitan areas, as urban layouts and artificial surfaces significantly exacerbate local thermal environmental stress. A large number of epidemiological literatures clearly confirms a robust correlation between long-term heat exposure and elevated mortality and morbidity; The main driving factors are acute cardiovascular and respiratory failure.[4-6] Furthermore, studies have shown that severe heat waves can lead to kidney related deaths and trigger emergency hospital admissions for high-risk elderly populations.[7,8] Accordingly, optimizing outdoor thermal comfort at the pedestrian level has become the core cornerstone of contemporary climate adaptive urban planning and design frameworks.

In response to increasing urban heat stress, numerous studies have investigated strategies to improve outdoor thermal comfort at pedestrian level.[9-13] Because pedestrians are directly exposed to outdoor climatic conditions, thermal comfort assessment has become an important component of urban environmental research. Various thermal indices have been developed to evaluate outdoor thermal environments, including the Universal Thermal Climate Index (UTCI) and Physiological Equivalent Temperature (PET).[14-15] Among these indices, PET and UTCI are currently the most widely adopted indicators for evaluating outdoor thermal comfort under dynamic environmental conditions. Recent advances have also enabled the quantification of pedestrian thermal comfort using 360° street view factors and UTCI-adjusted pedestrian accessibility analysis, providing more comprehensive assessment frameworks.[16-17] Researchers found a significant correlation between PET and heat-related mortality.[18-20] PET index was put forward in 1999 as a universal index for the biometeorological assessment of thermal comfort. It is based on the Munich Energy-balance Model for Individuals (MEMI), which assesses the human thermal state in a physiologically relevant way.[21] It could be described as the indoor temperature where the human body undergoes a degree of thermal stress equals to the one in the outdoor environment.[20] The classifications of thermal perception are from Very Cold to Very Hot. PET has been widely adopted in studies of outdoor thermal comfort, urban microclimate assessment, and pedestrian thermal stress in China and other regions.[12,22] Long-term PET trend analysis has also been conducted in various regions to evaluate the changing thermal environment over decades.[23]

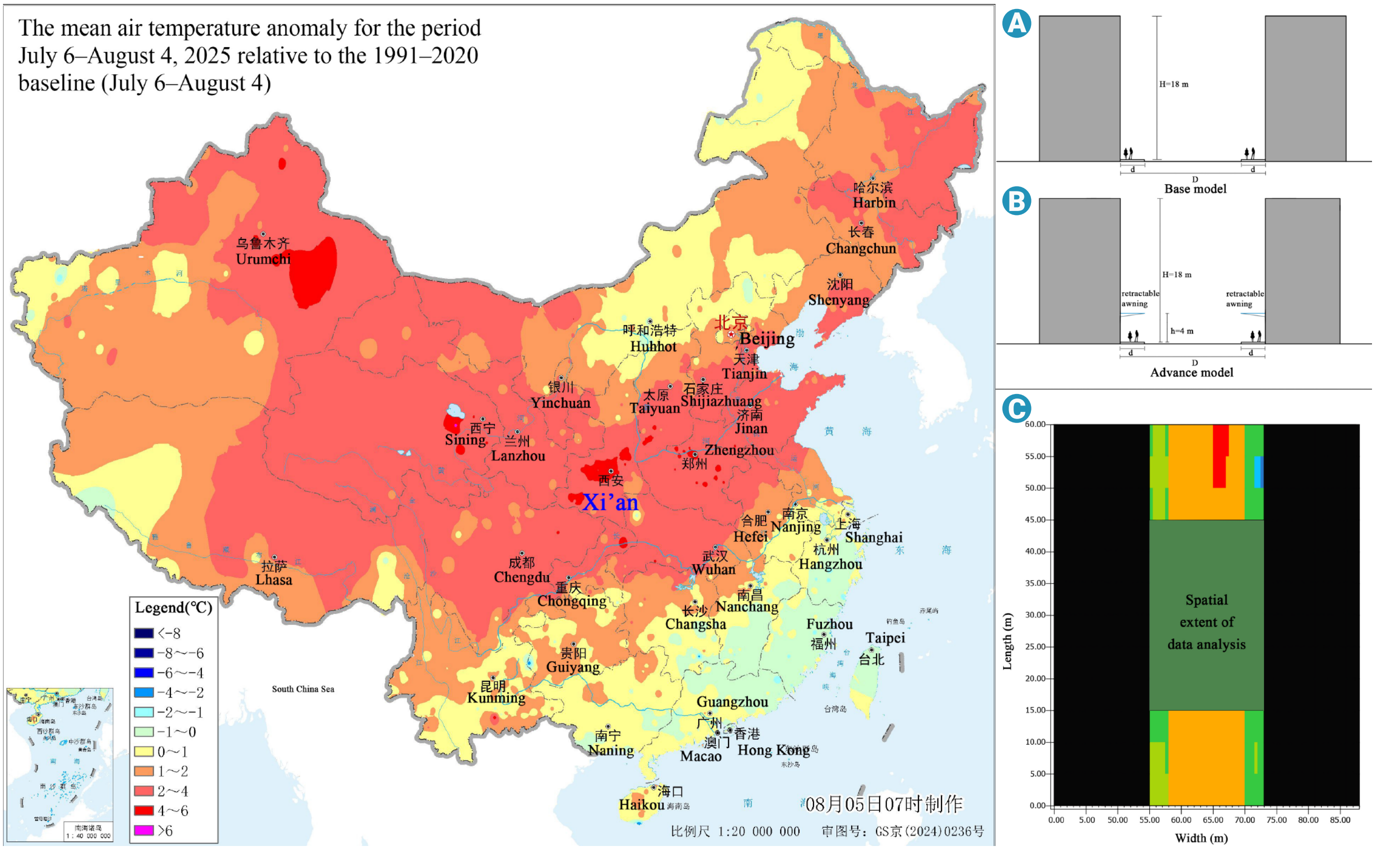

Figure 1. Location of Xi'an and the mean air temperature anomaly for the period July 6-August 4, 2025, relative to the 1991-2020 WMO baseline (July 6-August 4) (data source:National Climate Centre, https://cmdp.ncc-cma.net/cn/index.htm) Elevation schematic diagrams of research models and schematic diagram of simulation models (D = 18m north-south case)

Meanwhile, a large number of studies have explored urban heat mitigation through vegetation, cool materials, reflective surfaces, urban morphology optimization, and neighborhood-scale design strategies.[24-28] Building façade materials have also been identified as an important factor affecting outdoor thermal comfort and urban heat island intensity.[29] Although these approaches have demonstrated positive impacts on pedestrian thermal environment, relatively limited attention has been paid to the thermal effects of sunshade canopies along urban streets. sunshade canopies, especially retractable sunshade canopies, are common architectural elements in traditional commercial districts, where they provide shading and improve pedestrian microclimatic conditions. However, their quantitative cooling performance has rarely been investigated in northern Chinese cities under contemporary urban conditions, especially during extreme heatwave events.[30]

Urban microclimate conditions are closely correlated with the energy use of buildings. In periods of intense summer heatwaves, compact urban street canyons trap large amounts of solar radiation. This leads to a sharp rise in ambient air temperature and greater sensible heat accumulation on building exterior surfaces. Such thermal interactions inevitably raise indoor cooling demands and reduce the operating efficiency of on-site air conditioning systems. The summer of Northen China is becoming hotter, and the citizens are suffering extreme heat wave. Sustained extreme heat has led to a sharp rise in building cooling energy demand. For example, from 2024 to 2025, the daily maximum power load of Shaanxi province's power grid repeatedly set new records during summer heatwaves. The peak load reached 44.91 million kilowatts in 2025, with air conditioning electrical energy consumption accounting for roughly 33% of the total consumption.

Retractable sunshade canopies installed on buildings along urban residential streets deliver two-fold advantages. These structures offer effective shading for people on the street, and block horizontal and slanting solar radiation before it reaches lower building facades. In this way, they help regulate the overall thermal conditions of local microenvironments and support urban energy conservation. So, this present work focuses on the quantitative cooling effects of buildings sunshade canopies along streets on the surrounding pedestrian thermal environment and take the city of Xi'an, which is located in cold area of North China and becomes one of the ten hottest cities in China in summer, as a case study. In this research, Since the simulation results indicate that retractable sunshade canopies exert negligible impacts on wind speed (WS) and relative humidity (RH) at pedestrian level, this study only adopted air temperature (AT), mean radiant temperature (MRT) and physiological equivalent temperature (PET) to assess the variations in the thermal environment.

MATERIALS AND METHODS

Case area and climate

China, as the largest developing country in the current world, which has experienced rapid urbanization in the past decades. The majority of Chinese cities and their population expanded several times, making this country to be the largest contributor to the emissions of greenhouse gases currently. Extreme heat weather occurs more frequent in recent years, doing harm to human health and social activities. Some research revealed that by 2030, China will add at least 200 million new urban residents and be pushing against deadly heat waves due to climate change by the latter part of this century.[31] According to 2025 China Climate Bulletin, the average air temperature of 2025 (10.9 °C) is 1.0 °C higher than that of 1991-2020 (9.9 °C) (China Climate Bulletin 2025). Figure 1 shows that in July6-August4 2025, the average air temperature in most area of China is higher than that of 1991~2020, the maximum difference can reach 4~6 °C.

Xi'an is located in the Guanzhong basin, between east longitude 107°40 '~ 109°49' and north latitude 33°. As of the end of 2024, the built-up area of Xi'an City was 810.0 km^2, and its permanent resident population stood at 13.0658 million. As the urban construction has developed rapidly since China Reform and Opening Up and is still continuing ongoing process of urbanization, more constructions will be built, and large numbers of people will flock to the urban area in the future. However, the urban climate has changed drastically along with the process of urbanization in the past decades. In the year of 2025, the maximal air temperature has reached 42 °C and the number of hot days, In Xi'an, the summer of 2025 witnessed the hottest Sanfu period on record. Two extremely severe regional heatwaves struck the city in quick succession: the first during July 11-19, 2025, and the second during July 23-August 7, 2025. Notably, the July 23-August 7 heatwave episode recorded the longest duration in local meteorological history. The thermal environment is getting worse, doing harm to the dense population.

Simulation tool and calibration

ENVI-met developed by Michael Bruse is selected as the simulation software to carry out this study. Now, it is one of the most widely employed Computational Fluid Dynamics tool for outdoor thermal environment.[31–32] And our team have validated it is suitable for the local climate by the method of comparing simulation data with field measured data.[33–34] It is adopted to simulate the models in this study.

Model simulation

Case model description. This study takes typical street canyon spaces in Xi'an Old City (the area enclosed by the Ming Dynasty city wall) as a case study to investigate the quantitative impacts of retractable sunshade canopies on the thermal environment of street spaces. The selection of streets in Xi'an Old City as the target case is primarily based on the following considerations:

First, the Old City is located in the city center, where heat is difficult to dissipate, leading to frequent high-temperature events. Second, streets in the Old City accommodate high-density slow-moving traffic and daily activities of residents, resulting in extremely high health risks associated with heat exposure for the population. Third, the Old City faces the practical dilemma of extreme scarcity of available green space, making traditional greening strategies difficult to implement. Therefore, exploring how to improve the thermal environment of street canyons through refined regulation of sunshade canopies without altering the existing two-dimensional land use layout has urgent practical needs and guiding significance for the current micro-renovation-oriented urban stock renewal. This study focused on the effects of sunshade canopies along the streets on the surrounding pedestrian thermal environment.

Three common streets were extracted from existing urban streets to serve as the baseline models. The directions of the streets are north-south and east-west. The lengths of the streets are 60 m. The heights of the buildings, which are represented by H in Figure 1, along the streets are all 18m. The street widths, which are represented by D in Figure 1, of the models are 12m, 18m and 24m, very common widths in old urban area of Xi'an. While the length of sunshade canopies, which is represented by d, change a lot and the common length of 1.0m, 1.5m, 2.0m, 2.5m and 3.0m are applied to the case models (Figure 1A). As the base models have no sunshade canopies, so there are three basic cases of south-north and east-west corresponding to the three types of D values. Then optimized models are built with sunshade canopies based on the baseline models. The heights of sunshade canopies are 4m, which is the common height of ground floor (Figure 1B). Three values of D times five values of d, so fifteen optimized models and three baseline models were established for both north–south oriented streets and east–west oriented streets.

Simulation settings. ENVI-met is used in the current study. The unit grid size is 0.5 m (x axis) × 0.5 m (y axis) × 2 m (z axis) in the models. The models began to run at 16:00 on 20 June and lasted 32 hours, so they finished on 21 June. The data of PET on 21 June were exported from the software and analyzed. As 21 June is Summer Solstice with the highest solar angle throughout the whole year. The main input simulation parameters are shown in Table S1 and Table S2, which were obtained from the Typical Meteorological Year (TMY).

The first few hours were used to warm up the software and then the hourly data from 6:00 to 20:00 were collected as people's outdoor activities are mainly carried out during this period and the thermal environment have significant impacts on human health. The values were chosen at 1.4 m height as it's pedestrian level and the thermal environment has the most significant effects on the human thermal sensation. In order to eliminate the impact of model boundary, only the data of middle section were chosen, as the colored section shown in Figure 1C. The data of the space with and without sunshade canopies were chosen respectively.

RESULTS

Effect evaluation in the result analysis was conducted using the difference between the results of the optimized model and the baseline model. Therefore, a negative difference ($\Delta < 0$) indicates that the value of the optimized model is lower than that of the baseline model, meaning that the sunshade canopy exerts a positive thermal environment improvement effect. Conversely, a positive difference indicates a negative effect. The analysis results for east-west oriented streets and north-south oriented streets are presented separately in the following sections.

Hourly AT variation

The results of east-west oriented streets show that sunshade canopies can effectively reduce air temperature ($\Delta AT < 0$) throughout the daytime period (6:00–20:00), and the overall cooling magnitude increases with the extension length d of the sunshade canopy. However, this cooling performance exhibits significant spatial scale dependence in street canyons. In the 12 m narrow street canyon, the temperature control effect of sunshade canopies is the most pronounced, reaching a global maximum cooling reduction of -1.64°C at 11:00 (d = 3.0 m), and maintaining a high-efficiency cooling of above -1.3°C during the high-temperature daytime period from 10:00 to 16:00. In contrast, as the street canyon width increases to 18 m and 24 m, the amelioration effect of sunshade canopies on air temperature is significantly weakened, with the maximum cooling reductions converging to -1.21°C (14:00–15:00) and -0.56°C (15:00), respectively (Figure 2).

The underlying microclimatic mechanism of this phenomenon lies in that the solar geometric characteristics of east-west oriented street canyons determine the illuminated area of the underlying surface. Due to its high height-to-width ratio (H/W), sunshade canopies in the 12 m narrow street canyon can efficiently cover and block the heating of south and north building facades and adjacent ground pavement by direct solar radiation, significantly inhibiting the transfer of sensible heat flux to the street canyon air. In the 24 m wide street canyon, however, the low H/W ratio results in a large area of the underlying surface being exposed to core direct sunlight. The projection area of limited-length sunshade canopies (d ≤ 3.0 m) accounts for an extremely low proportion of the total street surface, and combined with intense ambient air convective mixing, their temperature control effect is severely diluted, leading to a relatively flat diurnal cooling curve (Figure 2).

Notably, an abnormal reversal occurs in the 12 m street canyon during the early morning (6:00–7:00), where short sunshade canopies (d = 1.5 m, cooling reduction -0.39°C) outperform long sunshade canopies (d = 3.0 m, cooling reduction -0.20°C). This is attributed to the obstruction of weak air convection and the inhibition of local nocturnal cold air dissipation in the narrow street canyon by the ultra-long canopy cover during early morning hours (Figure 2).

In north-south oriented streets, sunshade canopies all exert positive local cooling effects, but their temperature control performance exhibits strong nonlinear characteristics and spatial scale dependence. In the 12 m narrow street canyon, the temperature control mechanism of sunshade canopies shows a unique "bimodal" non-monotonic trend: during the high-temperature daytime period from 11:00 to 16:00, the cooling effect increases significantly with the extension length d of the sunshade canopy, reaching a maximum cooling reduction of -1.03°C at 13:00 (d = 3.0 m). In contrast, during the early morning (6:00–10:00) and evening (18:00–20:00), medium-length sunshade canopies (d = 1.5 m, maximum cooling reduction of -0.51°C) outperform ultra-long sunshade canopies (d = 3.0 m, cooling reduction of only approximately -0.13°C) (Figure 3).

This microclimatic phenomenon can be attributed to the coupling effect of the unique solar geometric characteristics of north-south street canyons and the microenvironment of narrow street canyons: during dawn and dusk periods, narrow street canyons with high H/W have strong self-shading capacity, and direct sunlight cannot penetrate to the pedestrian level. At this time, extending the sunshade canopy cannot provide additional shading benefits. Conversely, sunshade canopies with a total extension of 6 m on both sides severely limit the sky view factor (SVF) of the street canyon, hinder the nocturnal dissipation of longwave radiation from the underlying surface and inhibit convective heat dissipation by air flow, leading to local accumulation of heat beneath the canopy cover (Figure 3).

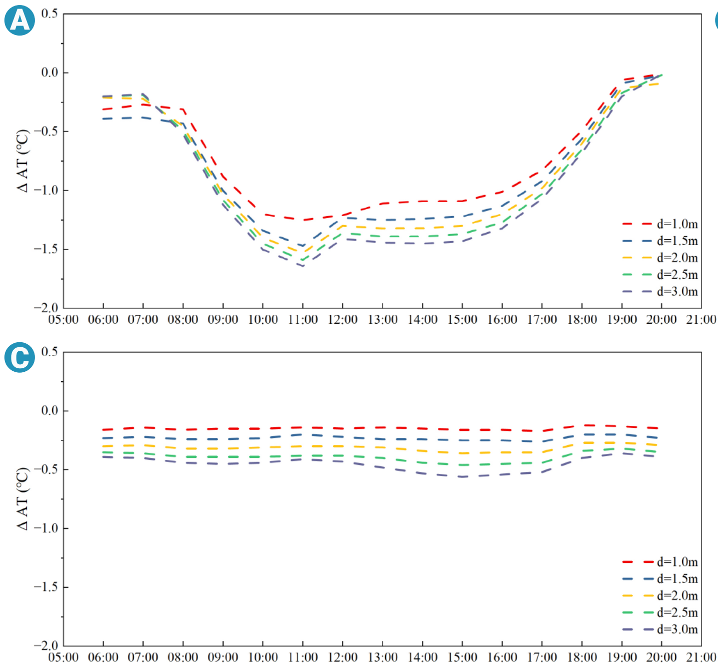

Figure 2. East-west air temperature variation:(A) D=12m, (B) D=18m, (C) D=24m.

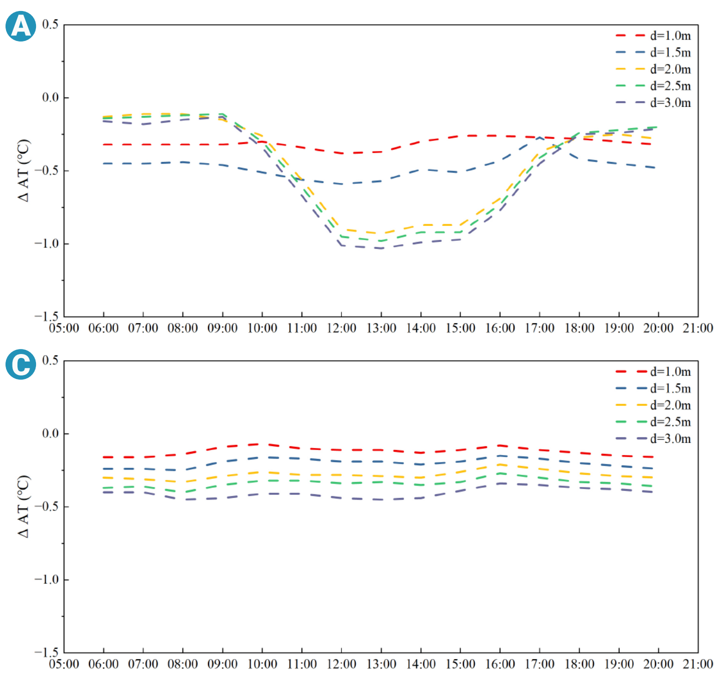

Figure 3. North-south air temperature variation:(A) D=12m, (B) D=18m, (C) D=24m.

As the street width increases to 18 m and 24 m, the cooling pattern of sunshade canopies reverts to the traditional characteristic of monotonic increase with length d. However, due to the expanded street canyon volume, increased unshaded area and intensified convective mixing, the overall temperature control effect is significantly diluted, with the maximum cooling reduction in the 24 m wide street canyon converging to -0.45°C (13:00) (Figure 3).

Hourly MRT variation

Simulation results of the east-west streets indicate that during the monitoring period from 6:00 to 20:00, the implementation of sunshade canopies generally induces significant negative ΔMRT responses, and their thermal environment mitigation potential exhibits highly sensitive nonlinear coupling characteristics with sunshade canopy extension span (d), street canyon H/W, and diurnal solar geometric path. First, under all street width scenarios, the MRT reduction magnitude shows a strictly monotonic positive correlation with sunshade canopy span. As d increases from 1.0 m to 3.0 m, the radiation regulation gain increases incrementally and reaches the global optimum at d = 3.0 m. This is attributed to the fact that large-span overhangs effectively reduce the SVF at the pedestrian open level, achieving the interception of high-intensity direct shortwave radiation through large-area continuous physical shadows. However, this radiation shielding efficiency is severely constrained by the geometric scale of street canyons. In this narrow street canyon, which is only 12 meters wide, sunshade canopies exhibit significant radiation attenuation capacity. Specifically, a peak ΔMRT of -12.61°C is recorded at 8:00 under the maximum canopy extension (d = 3.0 m). As the width of the street increases from 18 meters to 24 meters, the aspect ratio of the canyon decreases, and the local radiative cooling effect significantly

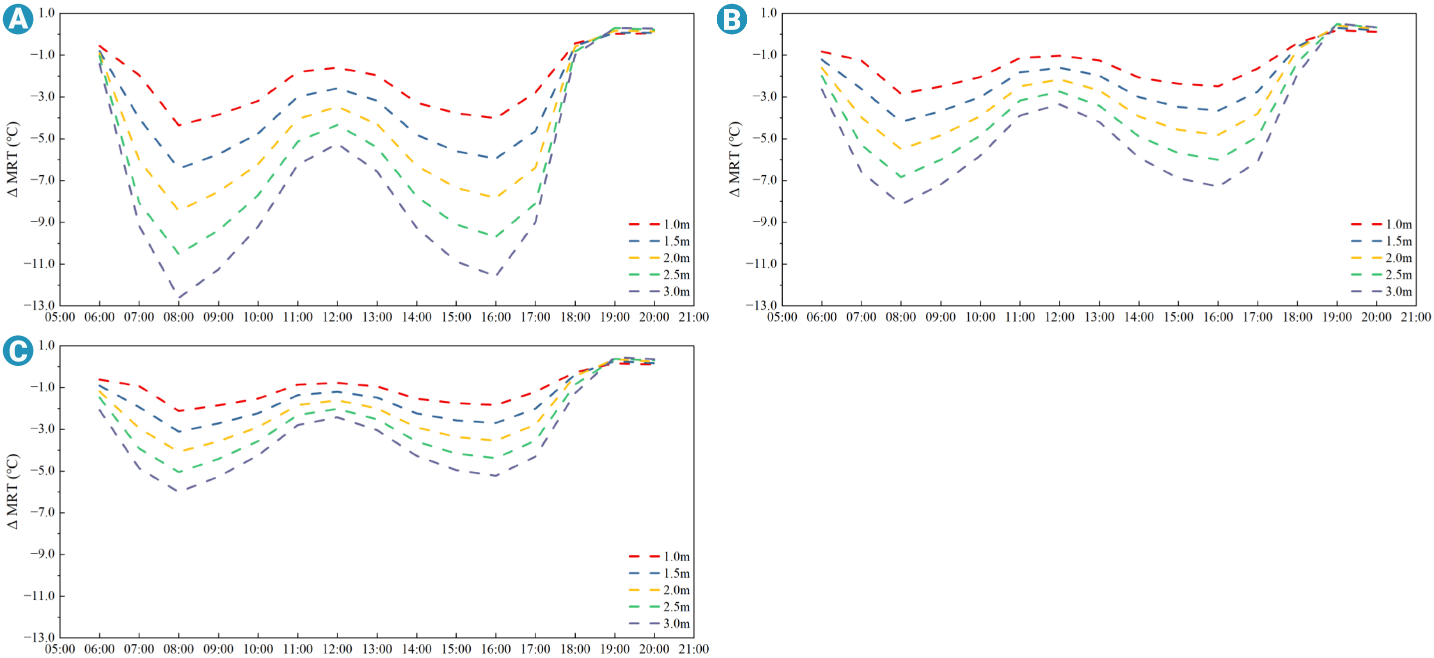

Figure 4. East-west MRT variation:(A) D=12m, (B) D=18m, (C) D=24m.

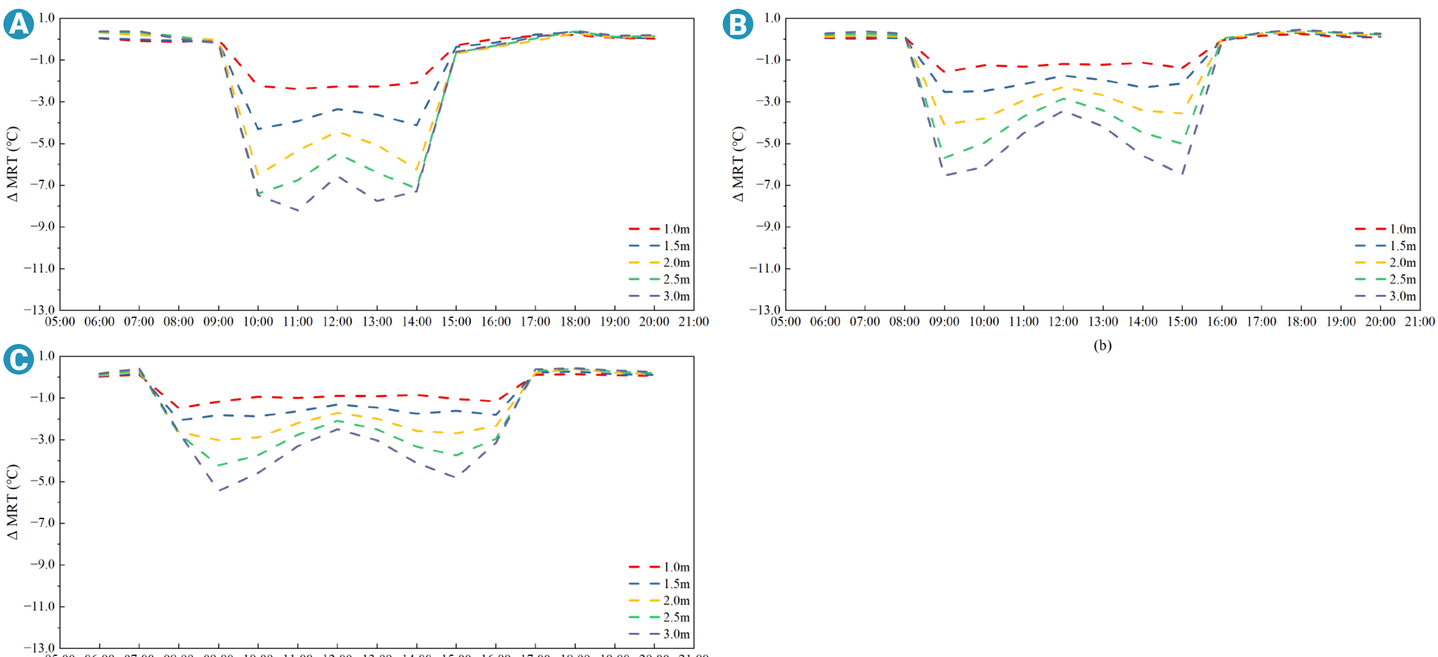

Figure 5. North-south MRT variation:(A) D=12m, (B) D=18m, (C) D=24m.

weakens with the maximum ΔMRT values dropping to -8.15°C and -6.01°C at 8:00, respectively. This spatial variation indicates that expansive, highly open street geometries can lead to long-term exposure of large areas of impermeable pavement to direct sunlight. Therefore, the huge amount of solar radiation across the street core severely dilutes the microclimatic thermal shelter benefits generated by the surrounding shading facilities set along the building facade (Figure 4).

In all north-south oriented street canyons, the attenuation magnitude of ΔMRT values monotonically increases with d value and achieves maximum effects at d = 3.0 m. From a spatial distribution perspective, the radiant cooling performance of these cantilever structures shows a clear trend of diminishing marginal returns as street width increases. The narrow street with a width of 12 meters records a global peak ΔMRT of -8.20°C at 11:00, whereas the maximum temperature drops within the 18 m and 24 m configurations are limited to -6.53°C and -5.45°C, respectively (both occurring at 9:00). This significant spatial heterogeneity arises from the dynamic coupling relationship between the geometric position of the sun and the axial direction of north-south streets. It is precisely due to the interaction of these geometric factors that the 12 m narrow canyon can continue to maintain a strong and high-intensity radiative cooling effect even during the high solar altitude period from 10:00 to 14:00 (Figure 5).

In contrast, the 18 m and 24 m wide street canyons show a distinct bimodal characteristic: the main cooling peaks are precisely concentrated in the early morning (9:00) and late afternoon (15:00), while the improvement magnitude drops significantly at noon (12:00). This is because at noon, solar rays with high altitude angles are nearly parallel to the north-south orientation and directly irradiate the center of the street canyon, exposing large areas of hard pavement and preventing the projection of horizontal sunshade canopies from covering the core pedestrian area. In contrast, during the early morning and late afternoon with low solar altitude angles, overhanging

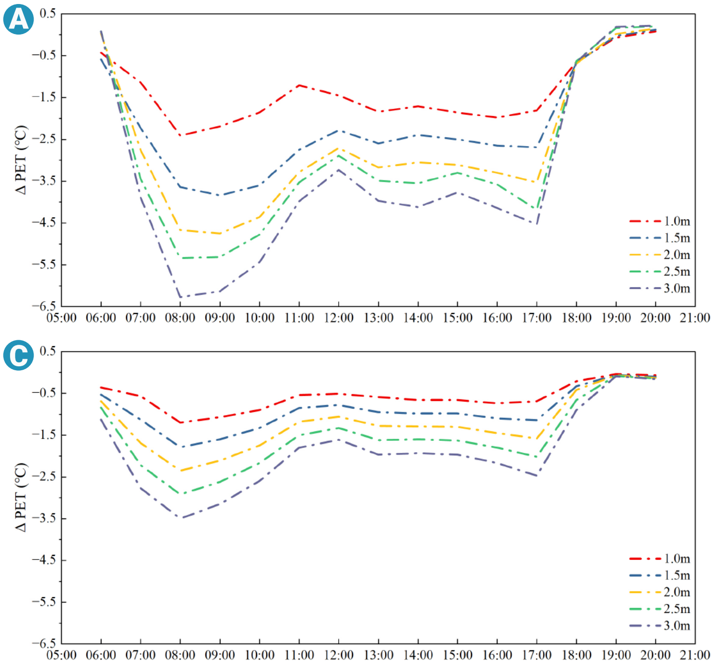

Figure 6. East-west MRT variation:(A) D=12m, (B) D=18m, (C) D=24m.

canopies can efficiently intercept oblique direct shortwave radiation from the side facades. Similarly, during early morning and nighttime, since the canopies reduce the SVF and hinder the longwave radiation heat dissipation from the underlying surface to the cold sky, a slight warming effect is generally induced (Figure 5).

Hourly PET variation

The sunshade canopies exhibit significant cooling benefits during most daytime hours in the east-west streets, and their microclimate improvement performance is highly dependent on the nonlinear coupling relationship among d, D, and diurnal solar geometric path. Overall, under all street configurations, the reduction magnitude of PET increases incrementally with the extension of sunshade canopy span, reaching the global peak at d = 3.0 m, which reveals the strong interception effect of deep shading on direct solar radiation. Spatially, the sensitivity of street microclimate to shading intervention decreases significantly with the reduction of H/W ratio (i.e., street widening): in the 12 m wide narrow street canyon, the maximum PET reduction induced by sunshade canopies reaches as high as -6.27°C (8:00, d = 3.0 m); when the street width expands to 18 m and 24 m, the maximum PET differences converge to -4.68°C and -3.50°C, respectively, indicating that the high openness of wide street canyons weakens the relative thermal comfort benefits of lateral shading facilities (Figure 6).

The cooling trend in the east-west canyon shows a clear bimodal diurnal variation pattern. The main cooling peak occurs in the early morning (around 8:00), followed by a second peak in the evening (16:00-17:00). On the contrary, there is a significant local decrease in shading efficiency around noon (12:00), for example, during this period, the maximum temperature drops in a 12-meter-wide canyon is limited to ΔPET of -3.23°C. This temporal distribution is essentially determined by the unique solar azimuth angle of east-west oriented street canyons—at noon, high-altitude solar rays irradiate the center of the street canyon vertically, causing the effective projection height and coverage area of horizontal building canopies to plummet to the minimum. In contrast, during the early morning and late afternoon with low solar altitude angles, the canopies can maximally intercept low-angle incident direct solar radiation (Figure 6).

Sunshade canopies can effectively reduce PET values during the period from 6:00 to 20:00 in north-south streets, and their thermal environment regulation capacity is significantly modulated by d, D, and spatial solar geometric fluctuations. First, under all street width scenarios, the reduction magnitude of PET exhibits a clear positive correlation with d, i.e., it increases significantly with the increase of d value and reaches the optimal improvement effect at d = 3.0 m. This is mainly attributed to the fact that large-span shading facilities effectively block direct solar radiation and expand the projected shading area at the pedestrian level. Second, street geometric H/W imposes a critical constraint on the microclimate regulation performance of sunshade canopies. In the 12 m wide narrow street canyon, sunshade canopies exhibit the optimal cooling potential, with the maximum PET difference reaching -4.02°C at 13:00 (d = 3.0 m). As the street width expanded to 18 meters and 24 meters, the peak cooling magnitudes ΔPET decrease to -3.8°C and -3.11°C, respectively (both recorded at 9:00 under d = 3.0 m). This spatial decay phenomenon indicates that the high morphological openness characteristic of wide streets severely weakens the microclimatic thermal comfort benefits brought by surrounding shading facilities (Figure 7).

Daily mean AT, MRT and PET variation

Shown in Figure 8. For east–west oriented streets canyons, street width and the length of building-mounted retractable sunshade canopies exert a significant nonlinear combined driving effect on the daily mean air temperature improvement (ΔAT) at pedestrian height. The overall response surface presents a smooth, saddle-shaped topology, with the maximum thermal mitigation effect is concentrated at the geometric intersection of the minimum D (12 m) and maximum d (3.0 m). According to surface gradient analysis, the slope along the D axis is significantly steeper than that along the d axis, demonstrating that the canyon H/W is the main boundary condition determining the temperature regulation efficiency of the building shading system. Within the narrow 12 m street, the limited horizontal profile restricts naturally exposed surface area. Therefore, setting up a sunshade horizontally can quickly maximize the interception effect of direct solar radiation and effectively suppress the transfer of sensible heat flux to the urban canopy. On the contrary, expanding the street width to 24 meters will cause the response surface to sharply flatten. Within this expansive geometry, extending the canopy from 1.0 m to its 3.0 m upper limit yields negligible microclimatic returns, with the diurnal ΔAT shifting merely from −0.14 °C to −0.45 °C.

Three-dimensional response surface analysis demonstrates that street width and d also produce prominent nonlinear synergistic effects on daily mean ΔAT for pedestrian layers in north–south street canyons. Contrary to conventional cognition that narrow 12 m canyons with minimum exposed area deliver optimal cooling, the global optimum for thermal regulation locates at the coupled configuration of moderate 18 m street width and full 3.0 m sunshade canopy length (ΔAT = −0.65 °C). For 12 m canyons, progressive canopy extension drastically reduces SVF via bilateral overhangs, blocking nocturnal and crepuscular longwave radiative dissipation as well as

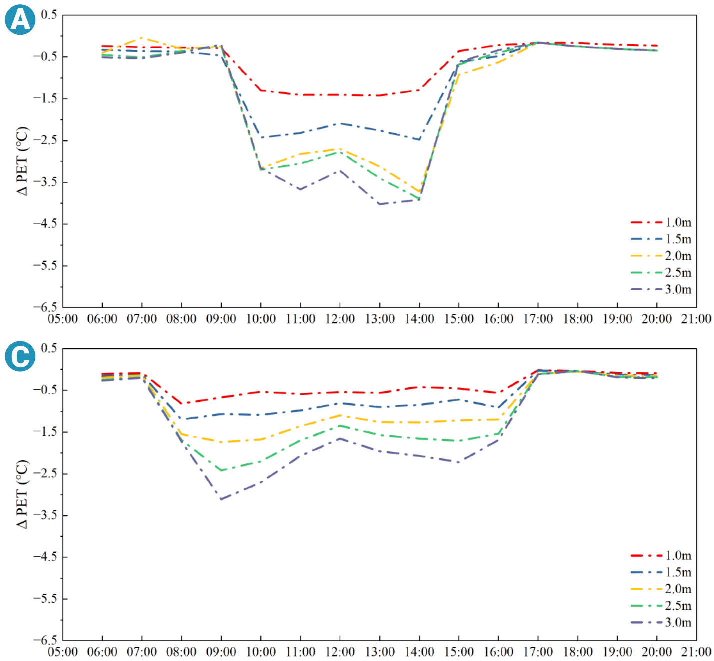

Figure 7. North-south PET variation:(A) D=12m, (B) D=18m, (C) D=24m.

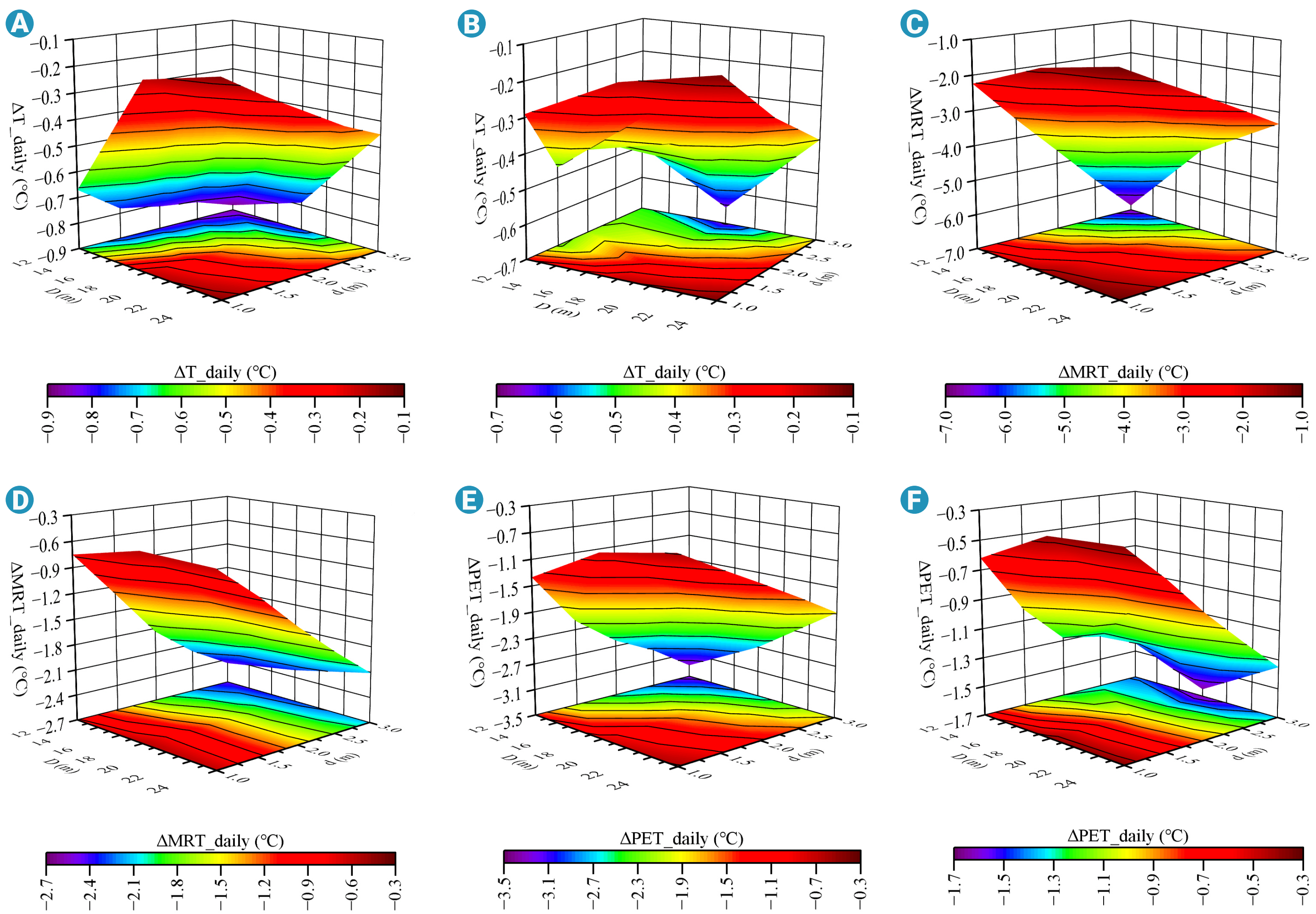

Figure 8. Response surface of daily mean air temperature difference (°C) as a function of D and d: (A) for east-west streets, (B) for north-south streets. Response surface of daily mean radiant temperature difference (°C) as a function of D and d: (C) for east-west streets, (D) for north-south streets. Response surface of daily mean physiological equivalent temperature (°C) as a function of D and d: (E) for east-west streets, (F) for north-south streets

convective heat exchange and triggering the heat-trapping effect; accordingly, cooling benefits fluctuate non-monotonically. In comparison, enlarged canyon volume at 18 m facilitates sufficient ventilation pathways to eliminate heat accumulation, allowing long canopies to maximize their advantages in intercepting secondary reflected radiation. For extra-wide 24 m canyons, excessive canyon openness leads to diminishing marginal returns of shading cooling. The dataset confirms a golden equilibrium between spatial canyon dimension and overhang span for microclimate optimization in north–south street canyons.

In the east-west streets, D and d have a highly significant and regular monotonic synergistic effect on the daily mean MRT at pedestrian level. Unlike air temperature, which is highly susceptible to wind speed and convective disturbances, the MRT response surface presents a highly regular and unidirectional tilted topological structure. The optimal global solution for radiation mitigation effect is located at the geometric intersection of the minimum street width of 12 m and the maximum tree crown extension length of 3.0 m, at which point the daytime average ΔMRT value reaches a peak of -6.86°C. Response surface gradient analysis shows that in all observation areas, ΔMRT displays a robust, bidirectional linear amplification, scaling positively with d and inversely with D. In the east-west canyon, the sun's trajectory is perpendicular to the street axis at noon, causing the bottom of the street canyon and the south facing building facades to be exposed to high-intensity direct solar radiation for a long time. When D increases from 12 meters to 24 meters, the unobstructed area of the opaque road surface expands, resulting in a significant increase in the longwave thermal radiation density in the core area of the street; This surge effect weakens the local cooling effect of the surrounding shading mechanism, reducing the maximum relief amplitude to -3.33 ° C.

In the north-south streets, D and d exert a significant synergistic interaction on daily mean ΔMRT, and the mitigation effect shows a monotonically increasing trend with the degree of d. The optimal configuration point is located at the geometric junction of a 12 m wide street and a 3.0 m sunshade canopy, which can achieve a peak ΔMRT value of -2.45 ° C. It is worth noting that the maximum radiation mitigation effect in this north-south street (-2.45 ° C) is still much lower than the results observed in the east-west street (-6.86 ° C). The key mechanism leading to this spatial heterogeneity stems from the daily dynamic changes in the geometry of the sun and street: the east-west facade can maximize the use of canopy shading effects due to continuous sunlight exposure. At noon, the trajectory of the sun is almost parallel to the north-south direction of the street axis, causing direct sunlight to penetrate vertically to the bottom of the street canyon at high solar elevation angles, severely weakening the shading effect of the sunshade canopy structure during peak radiation periods. In addition, the extremely small slope along D axis indicates that under north-south conditions, the impact of SVF changes caused by street width on daily cumulative radiation is negligible. On the contrary, the length of the shading canopy remains the main determining factor as it can effectively capture low angle lateral radiation during dawn and dusk periods.

In the east–west streets, the D and d exert a highly significant synergistic regulatory effect on the daily perceived temperature (ΔPET) at the pedestrian level. As a comprehensive biometeorological indicator that integrates air temperature, mean radiant temperature, and aerodynamic properties, the PET response surface exhibits a highly structured and monotonically inclined topological distribution characteristics. The optimal global solution for microclimate improvement is located at the geometric intersection of the minimum D (12 meters) and the maximum d (3.0 meters), which can reduce the daily average PET by 3.31 °C. Process-based analysis indicates that during summer daytime, east–west canyons are subjected to intense, superimposed high-flux direct solar irradiance and secondary longwave radiation emitted from south-facing building facades, which represent the primary drivers of pedestrian thermal discomfort. Process analysis shows that during summer daytime, east-west streets are simultaneously affected by strong superimposed high-throughput direct solar radiation and secondary longwave radiation emitted from southbound building facades, which are the main factors causing pedestrian thermal discomfort. The sunshade facilities installed on the building facade significantly alleviate extreme radiant loads through physical shielding, thereby optimizing human thermal balance. Conversely, as d expands from 12 m to 24 m, the proportion of unshaded impervious pavement increases, resulting in a maximum PET reduction of -1.88 °C. These research results imply that thermal comfort optimization for east–west street layouts should prioritize continuous, deep sunshade systems to maximize spatial coverage and enhance pedestrian microclimatic adaptability to extreme high temperatures.

For north–south oriented streets, D and d exhibit a pronounced nonlinear coupling effect on pedestrian-level PET mitigation. Response surface analysis shows the global optimal configuration is not the conventionally preferred 12 m narrow canyon, but an intermediate 18 m width combined with maximum d (3.0 m), achieving a peak daily PET reduction of -1.65 °C. In 12 m streets, extensive bilateral shading drastically reduces SVF, blocking direct midday solar radiation but also impeding nocturnal longwave radiative cooling and turbulent convective heat transfer. This induces a "heat-trapping" anomaly, limiting net cooling to only -1.44 °C at d = 3.0 m. In contrast, 18 m streets maintain sufficient ventilation to remove accumulated heat, fully realizing deep shading benefits. In 24 m streets, excessive openness causes convective thermal dilution, leading to diminishing returns with a peak PET reduction of -1.35 °C. Thus, north–south street microclimatic regulation requires a deliberate geometric trade-off between street aspect ratio and sunshade length.

CONCLUSIONS

This study used a full factor simulation matrix covering three typical street widths and five sunshade canopy lengths to quantify the hourly dynamic changes and daily evolution characteristics of three pedestrian level microclimate indicators - air temperature (AT), mean radiation temperature (MRT), and physiological equivalent temperature (PET). The main conclusions are as follows:

The three microclimatic indicators exhibit highly synchronized daily trends, but there are still mechanistic differences in the hourly variation patterns and peak response characteristics. Throughout the daily cycle 6:00-20:00, the mitigation effect of the shading elements on all indicators its peak globally during the period of highest solar radiation intensity. On the contrary, during the early morning and evening hours, the thermal protection effect will significantly weaken or trigger adverse microclimate impacts. Specifically, mean radiant temperature shows instantaneous geometric sensitivity to solar altitude angle, with the most dramatic decline in improvement magnitude occurring at 12:00–13:00 when solar radiation is strongest at noon. Air temperature, influenced by underlying surface thermal inertia and sensible heat release, exhibits a significant 1–2 hour thermal lag effect in its peak interval (13:00–15:00) compared to MRT. As a composite index, the hourly characteristics of physiological equivalent temperature are primarily dominated by MRT's thermal control during high-radiation daytime hours, while inheriting the convective regulation properties of AT during dawn and dusk (6:00–8:00, 18:00–20:00).

Microclimate regulation in east-west oriented streets conforms to a direct linear mapping of "full-time and hourly performance". In east-west street canyons, since the summer solar trajectory is parallel to the street orientation throughout the day, the installation of sunshade canopies can stably intercept high-flux direct shortwave radiation and secondary longwave radiation from building facades at every hour during the daytime. Its hourly improvement benefit increases monotonically with increasing sunshade canopy length, and its hourly and daily mean optimal solutions are highly consistent, both firmly locked at the geometric coupling point of the minimum street width (12 m) and maximum sunshade canopy length (3.0 m).

North-south oriented streets exhibit hourly nonlinear misalignment and "Heat Trapping" effects caused by "large-angle solar radiation penetration" at noon. In north-south street canyons, since the solar trajectory traverses above the canyon around noon, direct sunlight penetrates vertically to the canyon floor at large angles, leading to a significant attenuation of the interception efficiency of side-mounted sunshade canopies during the peak period of highest radiation energy density (12:00–13:00). Furthermore, during the high-temperature period in the afternoon (13:00–15:00) when underlying surfaces release stored heat, the combination of 12 m ultra-narrow street canyons and extra-long sunshade canopies (>1.5 m) drastically compresses SVF and impedes near-ground turbulent convection, preventing sensible heat dissipation and thus triggering a significant "Heat Trapping" effect on the hourly curves. Constrained by this, the global optimal solutions for air temperature and physiological equivalent temperature in north-south oriented streets do not appear in narrow canyons but shift outward to the intersection of moderate street width (18 m) and maximum sunshade canopy length (3.0 m).

The findings of this study provide important insights for establishing a synergistic regulation system between street microclimate and building energy-efficient cooling. The microclimatic modifications quantified in this study establish a direct thermodynamic link to the mitigation of space-cooling loads in adjacent building portfolios. Within narrow east-west oriented canyons, the prominent ambient temperature drop (ΔAT up to -1.64 °C) paired with the substantial radiative shielding (ΔMRT up to -12.61 °C) drastically attenuates the conductive and radiant heat flux entering ground-floor building envelopes during peak solar periods. This microenvironmental cooling effectively enhances the operational Coefficient of Performance (COP) of localized air conditioning condensers that reject heat directly into the street canyon space. Concurrently, the non-monotonic "heat-trapping" phenomenon discovered in narrow north-south canyons under full canopy deployment validates the energetic necessity of the "retractable" mechanism. This responsive framework successfully bypasses the overnight structural thermal penalties of static shading, presenting a highly scalable, passive climate-adaptive pathway to optimize urban block energy efficiency.

REFERENCES

1. Bongaarts J. (2024). IPCC, 2023: Climate Change 2023: Synthesis Report. *Popul. Dev. Rev.* **50**:577–580. DOI:10.1111/padr.12632
2. Qin P., Xie Z. and Jia B. (2026). Increasing exposure to compound heatwave and drought events in China during 1961–2020. *Atmos. Res.* **340**:109099. DOI:10.1016/j.atmosres.2026.109099
3. China Meteorological Administration, National Climate Committee. (2026). 2025 China Climate Bulletin. *China Meteorological Administration.*
4. Meehl G.A. and Tebaldi C. (2004). More intense, more frequent, and longer lasting heat waves in the 21st century. *Science* **305**:994–997. DOI:10.1126/science.1098704
5. Gao J., Sun P., Huang M., et al. (2026). The interplay of heatwaves, air pollution, and green space on all-cause mortality in older adults with diabetes mellitus: a national cohort study. *BMC Public Health* **26**:27606. DOI:10.1186/s12889-026-27606-8
6. Wu R., Zhang J., Luo Z., et al. (2026). Spatiotemporal evolution of heat health risks in megacities at the township and subdistrict scales: A case study of Chongqing's central urban area. *Urban Clim.* **67**:102920. DOI:10.1016/j.uclim.2026.102920
7. Htay W.Z., Ng S.F.C., Kim Y., et al. (2026). Heatwaves, Cold Spells, and Renal Disease Mortality in Japan: Vulnerable Populations and Temporal Trends. *Environ. Health* **4**:919–928. DOI:10.1021/envhealth.5c00468
8. Pinto A., Pennisi F., Borlini S., et al. (2026). Effects of Heat Waves on Hospitalizations, Emergency Department Visits, and Outpatient Care in Frail Older Adults: A Systematic Review and Meta-Analysis. *Diseases* **14**:176. DOI:10.3390/diseases14050176
9. Zhang J., Zhu G., Yin J., et al. (2024). Analysis of summer high temperature observations based on different sub surfaces. *Earth Sci. Inform.* DOI:10.1007/s12145-024-01439-8
10. Unal M. and Middel A. (2025). Improving thermal comfort in hot-arid Phoenix, Arizona courtyards: Exploring the cooling benefits of ground surface cover and shade. *Build. Environ.* **278**:113001. DOI:10.1016/j.buildenv.2025.113001
11. Bao J., Xu L., Shi Y., et al. (2023). The Influence of Street Morphology on Thermal Environment Based on ENVI-met Simulation. *ISPRS Int. J. Geo-Inf.* **12**:303. DOI:10.3390/ijgi12080303
12. Jayasinghe S., Jayasooriya V., Dassanayake M.S., et al. (2024). Effects of street tree configuration and placement on streetside thermal environment within a tropical urban canyon. *Int. J. Biometeorol.* **68**:1133–1142. DOI:10.1007/s00484-024-02653-1
13. Zou M. and Zhang H. (2021). Cooling strategies for thermal comfort in cities: a review of key methods in landscape design. *Environ. Sci. Pollut. Res.* **28**:62640–62650. DOI:10.1007/s11356-021-15172-y
14. Hoppe P. (1999). The physiological equivalent temperature - a universal index for the biometeorological assessment of the thermal environment. *Int. J. Biometeorol.* **43**:71–75. DOI:10.1007/s004840050118
15. Sargazi A.M., Heidari A., Davtalab J., et al. (2025). Comparative reliability assessment of PET and UTCI thermal comfort indices using Monte Carlo simulation. *Sci. Rep.* **16**:3431. DOI:10.1038/s41598-025-33440-6
16. Zhang M., Yan H., Wu R., et al. (2026). Quantifying pedestrian thermal comfort under extreme heat using 360° street view factors. *Sustain. Cities Soc.* **146**:107515. DOI:10.1016/j.scs.2026.107515
17. Aydin E.E., Chen Z., Ortner P.F., et al. (2026). Universal Thermal Climate Index (UTCI)-adjusted pedestrian accessibility: Urban design exploration for climate-resilience in tropical climates. *Sustain. Cities Soc.* **143**:107335. DOI:10.1016/j.scs.2026.107335
18. Borsi S.H., Khodadadi N., Khanjani N., Dastoorpoor M. (2021). Physiological equivalent temperature (PET) index and respiratory hospital admissions in Ahvaz, southwest of Iran. *Environ. Sci. Pollut. Res.* **28**:51888–51896. DOI:10.1007/s11356-021-14345-z
19. Ma X., Zhang L., Guo M., Zhao J. (2021). The effect of various urban design parameter in alleviating urban heat island and improving thermal health. *Environ. Sci. Pollut. Res.* **28**:38406–38425. DOI:10.1007/s11356-021-13179-z
20. Sharafkhani R., Khanjani N., Bakhtiari B., et al. (2020). The effect of physiological equivalent temperature index variations on mortality in Urmia (The Northwest of Iran). *Urban Clim.* **32**:100595. DOI:10.1016/j.uclim.2020.100595
21. Cui D.J., Zhang Y., Li X.Y., et al. (2022). Effects of different vertical façade greenery systems on pedestrian thermal comfort in deep street canyons. *Urban For. Urban Green.* **72**:127582. DOI:10.1016/j.ufug.2022.127582
22. Zhao H., Duan H., Wang Y., et al. (2026). A systematic review of outdoor thermal comfort research: Integrating climate zones, population groups, and methodological frameworks. *Sustain. Cities Soc.* **143**:107339. DOI:10.1016/j.scs.2026.107339
23. Roshan G., Yousefi R., Kovacs A., et al. (2018). A comprehensive analysis of physiologically equivalent temperature changes of Iranian selected stations for the last half century. *Theor. Appl. Climatol.* **131**:19–41. DOI:10.1007/s00704-016-1950-3
24. Shen P., Wang M., Ma H., et al. (2024). On the two-way interactions of urban thermal environment and air pollution: A review of synergies for identifying climate-resilient mitigation strategies. *Build. Simul.* **18**:1–21. DOI:10.1007/s12273-024-1210-X
25. Lee J., Kim M., Chon J. (2026). Street greenery design strategies to mitigate urban heat islands using the 2D and 3D streetscape indices. *Trees For. People* **23**:101111. DOI:10.1016/j.tfp.2025.101111
26. Priyadarshni P. and Pandey P. (2026). A footprint of UHI in India: a systematic review of causative factors, impacts and mitigation strategies. *Front. Sustain. Cities* **7**:1649138. DOI:10.3389/frsc.2025.1649138
27. Tsirigoti D. and Gkyrtis K. (2026). Recycled Pavement Materials and Urban Microclimate: Albedo and Thermal Capacity Effects on Heat Island. *Solar* **6**:5. DOI:10.3390/sol6010005
28. Mohsen A., Hassan S.T. and Mansoureh T. (2026). Evaluating the Efficiency of Materials and Vegetation in Enhancing Outdoor Thermal Comfort in Hot and Arid Climates. *J. Urban Plann. Dev.* 152(3). DOI:10.1061/jupddm.upeng-5781.
29. Jonathan R., Lin T., Lun I., et al. (2026). The impact of building façade materials toward outdoor thermal comfort and urban heat island. *IOP Conference Series: Earth Environ. Sci.* **158**:012011. DOI:10.1088/1755-1315/1582/1/012011
30. Zheng Z., Lin X., Chen L., et al. (2024). Effects of urbanization and topography on thermal comfort during a heat wave event. *Sustain. Cities Soc.* **102**:105233. DOI:10.1016/j.scs.2024.105233
31. Perini K., Chokhachian A., Dong S., Auer T. (2017). Modeling and simulating urban outdoor comfort: Coupling ENVI-Met and TRNSYS. *Energy Build.* **152**:373–384. DOI:10.1016/j.enbuild.2017.07.061
32. Tsoka S., Tsikaloudaki A., Theodosiou T. (2018). Analyzing the ENVI-met microclimate model's performance and assessing cool materials and urban vegetation applications-A review. *Sustain. Cities Soc.* **43**:55–76. DOI:10.1016/j.scs.2018.08.009
33. Yang Y.J., Zhou D., Wang Y.P., et al. (2019). Economical and outdoor thermal comfort analysis of greening in multistory residential areas. *Sustain. Cities Soc.* **51**:101730. DOI:10.1016/j.scs.2019.101730
34. Zhu Z.Z., Zhou D., Wang Y.P., et al. (2021). Assessment of urban surface and canopy cooling strategies in high-rise residential communities. *J. Clean. Prod.* **288**:125599. DOI:10.1016/j.jclepro.2020.125599

FUNDING AND ACKNOWLEDGMENTS

This research was supported by Natural Science Basic Research Program Project of Shaanxi Province (No. 2024JC-YBQN-0488), and Basic Scientific Research Projects of National Universities (No. D5000230151).

AUTHOR CONTRIBUTIONS

All authors contributed to the manuscript and approved the final version.

DECLARATION OF INTERESTS

The authors declare no competing interests.

DATA AND CODE AVAILABILITY

Data are available from the corresponding author upon reasonable request.

SUPPLEMENTAL INFORMATION

It can be found online at https://doi.org/10.59717/ipj.energy-use.2026.100058